Experimental and Numerical Analysis of Performance Discontinuity of a Pump-Turbine under Pumping Mode

X. Zhang[a], R. Burgstaller[b], X. Lai[a], A. Gehrer[b], A. Kefalas[b] and Y. Pang[a]

[a] School of Energy and Power Engineering, Xihua University, No.999, Jinzhou RD, 610039 Chengdu, China
[b] Andritz Hydro, Andritzer Reichsstrasse 68b, 8045 Graz, Austria

zhangxiang@mail.xhu.edu.cn

Abstract. The performance discontinuity of a pump-turbine under pumping mode is harmful to stable operation of units in hydropower station. In this paper, the performance discontinuity phenomenon of the pump-turbine was studied by means of experiment and numerical simulation. In the experiment, characteristics of the pump-turbine with different diffuser vane openings were tested in order to investigate the effect of pumping casing to the performance discontinuity. While other effects such as flow separation and rotating stall are known to have an effect on the discontinuity, the present studied test cases show that prerotation is the dominating effect for the instability, positions of the positive slope of characteristics are almost the same in different diffuser vane opening conditions. The impeller has principal effect to the performance discontinuity. In the numerical simulation, CFD analysis of tested pump-turbine has been done with k-ω and SST turbulence model. It is found that the position of performance curve discontinuity corresponds to flow recirculation at impeller inlet. Flow recirculation at impeller inlet is the cause of the discontinuity of characteristics curve. It is also found that the operating condition of occurrence of flow recirculation at impeller inlet is misestimated with k-ω and SST turbulence model. Furthermore, the original SST model has been modified. We predict the occurrence position of flow recirculation at impeller inlet correctly with the modified SST turbulence model, and it also can improve the prediction accuracy of the pump-turbine performance at the same time.

1. Introduction

Poor flow conditions such as rotating stall, back flow, flow recirculation and the like happened in the flow channel of the pump cause the positive slope of characteristics and lead to the instability of the whole system. Instability characteristics always fascinate researchers and engineers for a long time. A lot of research results have been achieved in respects of the cause of formation, mechanism, phenomenon, control method of instability characteristics. These results expand the operating range of pump and optimize the operating quality of pump. The unstable feature of pump characteristics results from the unstable complex flow accompanied by the backflow in the pump channel. The internal flow field of pump changes drastically when the pump operates in the condition which represents the positive slope of characteristics. It results in: 1) instability of system[1]; 2) break or sudden change of head, efficiency and power[2]; 3) worse pressure pulsation[3]; 4) greater risk of cavitation[4].

Current studies indicate the main reason of the unstable characteristics is that the rotating stall located impeller and diffuser, changing of velocity distribution at impeller outlet, backflow between impeller and pumping casing[5, 6, 7, 8].

As research continues, a more serious kind of positive slope characteristics went into our eyes. It is called the discontinuity characteristics. It is also manifested as hysteresis loop in pump characteristics. Kaupert K.A. did the first analysis of the hysteresis phenomenon of pump[2], but similar researches in the field of pump-turbine gave rise to more concerns[9]. Following the research method and idea of normal pump, researches on instability characteristics of pump-turbine had been done. The result is similar to former research on normal pump, that is the saddle characteristics results from backflow between impeller and diffuser[10].

As research method and technology improves, it is gradually found that not only rotating stall near impeller outlet and diffuser inlet but also recirculation at impeller inlet exist when the pump runs in the condition of performance discontinuity. Kaupert K.A.[11] found that the recirculation at impeller inlet was a strong stable flow structure in term of the experiment when performance discontinuity happened. Milan Sedlár[12] indicated that performance discontinuity is linked with impeller inlet recirculation by means of researches on the cavitation structure and its dynamics, NPSH characteristics of a high efficiency mixed-flow pump. More and more evidences demonstrated that the recirculation at impeller inlet has great effect on performance discontinuity.

This article focused on a pump-turbine model. Performance discontinuity of pump-turbine under pumping mode has been studied by means of experiment and numerical calculation.

2. Pump-Turbine Model

The specific speed n_s is 150 ($n_s = \frac{3.65n\sqrt{Q}}{H^{3/4}}$). The model is vertical single stage and single suction. This hydraulics is of a storage pump, thus has a shaft through the draft tube and can also operate in turbine mode. The number of impeller blades is 9, the rotating speed at test rig is 1200 RPM. The pumping casing is diffuser with volute. The principle meridional sketch drawing is shown below.

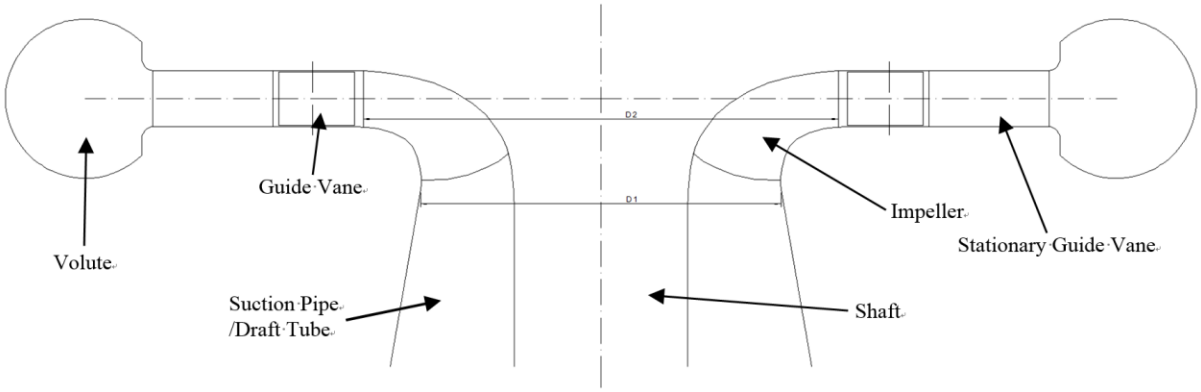

Figure 1. Meridional sketch drawing

3. Experimental Facility

Experiments were performed in ASTRÖ which is a hydraulic lab of ANDRITZ AG. The test stand is closed-loop arrangement. Its sketch picture is shown below. Its average error of efficiency is 0.25%, repeatability near optimum is equal or greater than ±0.1%.

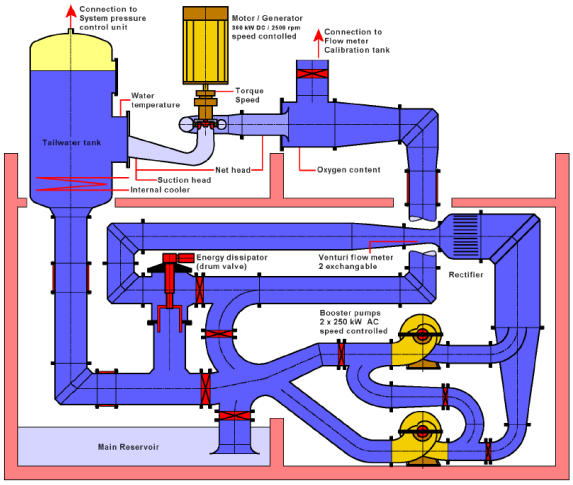

Figure 2. Sketch of test stand

4. Experiment and Results Discussions

A set of characteristics had been achieved in a series of diffuser vane openings. Flowrate-Head curves are shown in Fig. 3. Definitions of dimensionless coefficients are determined as follow:

Head coefficient: $\psi_2 = \dfrac{2gH}{U_2^2}$ (1)

Where H is the head of pump-turbine model, U_2 is the circumferential speed at impeller outlet.

Flowrate coefficient: $\phi_2 = \dfrac{v_{m2}}{U_2}$ (2)

Where v_{m2} is the meridional velocity at impeller outlet.

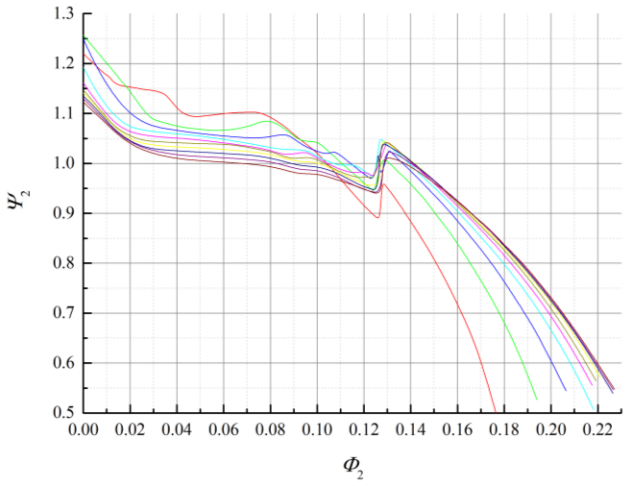

Figure 3. Flowrate-Head curves

Flowrate-head curves in conditions of 10 diffuser vane openings are presented in Fig. 3. They show that flowrate-head curves of model are the first-order derivative discontinuity, there are two cuspidal points in each curve. It means that a sudden change exits in flowrate-head curve. The head raises up abruptly as the flowrate is increasing. 10 flowrate-head curves with 10 diffuser vane openings are showed in Fig. 3 together. It is clearly presented that flowrates of performance discontinuity points are almost the same even if heads with different diffuser vane openings have great difference. In different diffuser vane openings, not only blade angels at diffuser vane inlet are difference but also areas of cross section of diffuser passage changes. Namely there are some different pumping casing if diffuser

vane openings are different. So the result of experiment illustrated that the performance discontinuity is independent of pumping casing, the impeller is the main role of discontinuity.

In the experiment we observed a phenomenon via transparent inlet section. When the flowrate was less than that of discontinuity point there was obvious inlet recirculation accompanied by loud noise and strong vibration. When the flowrate was more than that of discontinuity point the inlet recirculation disappeared, levels of noise and vibration get low.

The rotating stall which is originated from impeller and diffuser are normally considered as the reason of performance instability. But the onset of this kind of rotating stall is closely related to the geometry of diffuser such as occurred operating condition of rotating stall depends on the diffuser vane opening[13]. Moreover, the head drops relatively slowly if it is induced by the rotating stall, but in the present experiment heads changed rapidly i.e. breaking, it is so different from head changing situation in the rotating stall.

According to the analysis of characteristics and visual observation at inlet section, we found that the onset of inlet recirculation coincides with the performance discontinuity point. It is concluded presumably that the inlet recirculation has an important influence on performance discontinuity.

5. CFD Calculation and Discussions

In order to predict the onset flowrate of performance discontinuity and improve model design before model test, we need to do numerical simulation of internal flow field of model based on CFD method.

As we know from the result of the above section the performance discontinuity is independent of pumping casing. In the research result of Kaupert K.A.[2] it is said that the outlet reverse flow and any volute tongue flow interaction are not a necessary condition for the ψ-discontinuity. Thus the present paper paid attention to the impeller. Moreover, F. Ginter[15] indicated the flow instability being entirely impeller induced since that the measured impeller characteristics and that of the entire pump showed a performance discontinuity of nearly identical magnitude, located at the identical flowrate. In numerical studies of Masamichi Iino[14], Kaupert K. A.[2], F. Ginter[15] they showed that onset operating conditions of the performance discontinuity are the same when they were calculated in alone impeller or entire pump. The steady numerical simulation which is done in single impeller channel can also get an ideal result.

Authors had made a comparison of an impeller model without diffuser and the same model with diffuser, and found that impeller characteristics obtained by the model without diffuser compared with the model with diffuser are considered to be identical. Based on the above results, the incompressible steady flow simulation in a single impeller channel is carried out with the commercial CFD-code ANSYS CFX. The simulation domain is presented below.

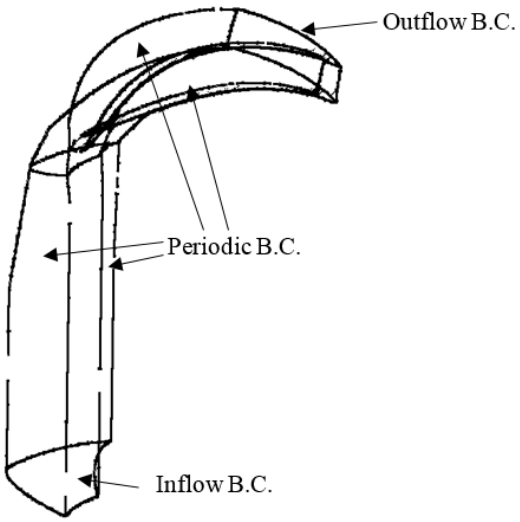

Figure 4. Simulation domain

The mass flow rate was given at inlet, flow direction is normal to inlet. The average static pressure is 0Pa at outlet. Periodic boundary conditions are shown in Fig.4. The entire calculation domain is rotating, the option of Alternate Rotation Model is enable.

Since the changing direction of flowrate is from small to large in the test, the larger flowrate calculation was performed by using the data previously calculated as the initial condition. Repeating this way, the flow fields were calculated at each flowrates.

The computational mesh is hexahedral structure grid. Three sets of meshes were used to check sensitivity of mesh. The number of cells are 302.2 thousand, 403.4 thousand and 806.8 thousand respectively. The same computational strategy were used, model characteristics and the length of inlet recirculation are almost the same. Considering the value of y^+ and the computational expense, the mesh with 403.4 thousand cells is the final choose. The average value of y^+ at blade surfaces is 11.87 in the design condition using SST turbulence model. F. Ginter[15] also refer to a more complex model, resolving the boundary-layer and simulating the unsteady interaction between impeller and volute, would include no additional information about the basic mechanism of the performance discontinuity, but only increase the computational time drastically. Fig.5 shows the computational mesh.

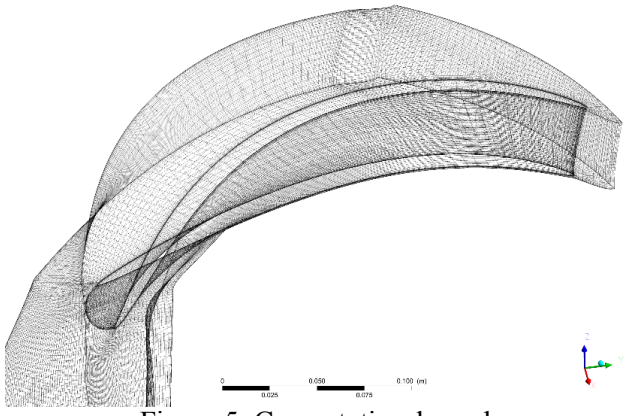

Figure 5. Computational mesh

The k-ω turbulence model and the SST turbulence model were used to close N-S equation respectively. The calculated Φ-ψ curves are presented below.

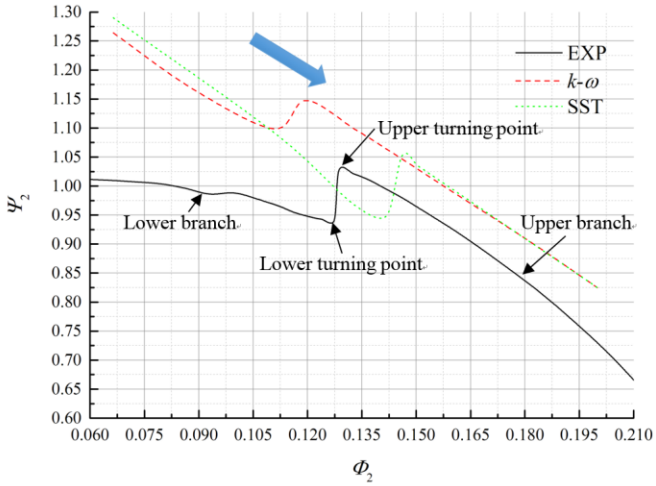

Figure 6. Φ-ψ curves

In Fig. 6 the solid line represents the test result at the design diffuser vane opening, the dash line is the result calculated using the k-ω turbulence model, the dot line is the result calculated using the SST turbulence model. Since the computational domain contains just the impeller, both of heads obtained by the k-ω model and the SST model are higher than the test result, and the head is better matched if the CFD model includes the diffuser vanes. We can find easily that both the k-ω turbulence model and

the SST turbulence model fail to predict the correct onset positon of the performance discontinuity. The k-ω turbulence model overestimates the onset of the inlet recirculation, the calculated position of the performance discontinuity is on the left of the test position. The SST turbulence model underestimates the onset of the inlet recirculation, the calculated position of the performance discontinuity is on the right of the test position. Referring to the results of this paper's references (mostly using the k-ε turbulence model), the calculated positions of the performance discontinuity are always on the left of their test results. Generally the SST turbulence model is better than the k-ε and the k-ω turbulence model, but it also predicts the onset position of the performance discontinuity incorrectly. Furthermore, authors have done this kind of calculation on other pumps and pump-turbines, there are no exception that the onset position calculated using the k-ω turbulence model is on the left of the test result, the onset position calculated using the SST turbulence model is on the right of the test result.

Situations of the inlet recirculation are shown in Fig.7~8. Flowrates of operating conditions referred to Fig.7~8 are listed in Table 1.

Table 1 Position of operating conditions (Φ_2)

Turbulence Model	Lower Branch	Lower Turning Point	Upper Turning Point	Upper Branch
k-omega	0.089	0.111	0.120	0.142
SST	0.111	0.142	0.146	0.164

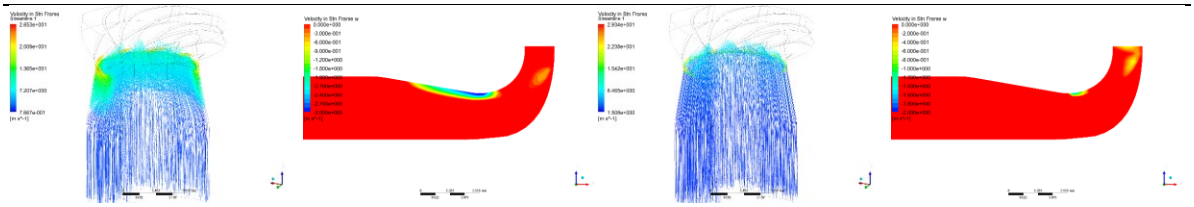

(a) Lower Branch (b) Lower Turning Point

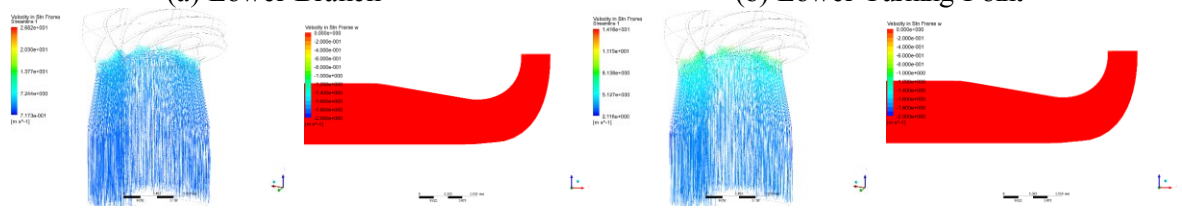

(a) Upper Turning Point (b) Upper Branch

Figure 7. Results of the k-ω turbulence model

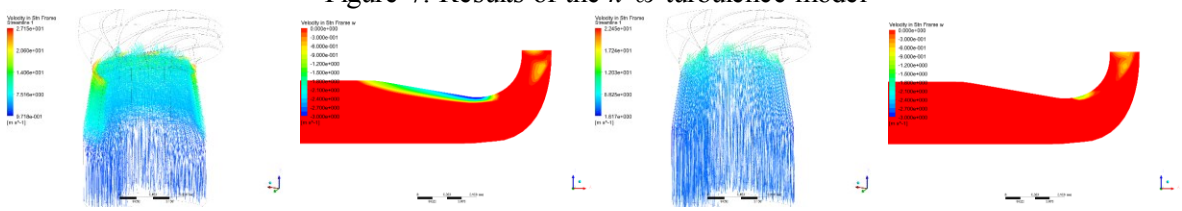

(a) Lower Branch (b) Lower Turning Point

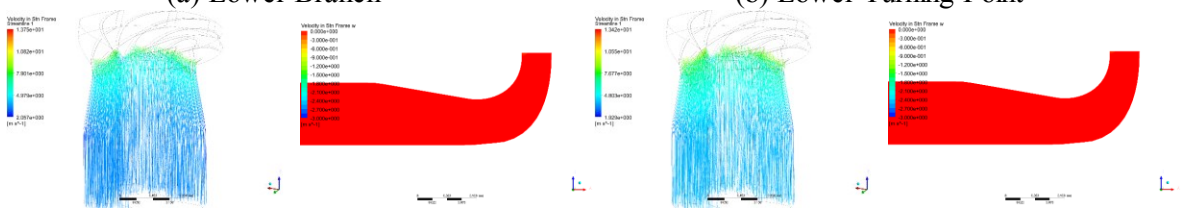

(a) Upper Turning Point (b) Upper Branch

Figure 8. Results of the SST turbulence model

In above pictures the absolute velocity streamlines are shown on the left side, the axial velocity contour is shown on the right side (the scale was adjusted for easy observation, the maximum velocity is set to 0 m/s). It can be found from pictures that the length of inlet recirculation is shorting while the flowrate is increasing, the length is almost 0 near the lower turning point, and there is no inlet recirculation from the upper turning point. It can be concluded that the inlet recirculation corresponds to the performance discontinuity directly.

The existing two-equation turbulence models cannot predict the onset of the performance discontinuity correctly according to references and authors' practice. Based on the above result, the essential issue is that the inlet recirculation cannot be calculated correctly by the existing two-equation turbulence models. If the more advanced turbulence model is used, we cannot afford the higher cost of the computation in the engineering application. And we had tried to use Reynolds stress model (steady and unsteady state), two-equation turbulence models with unsteady state as well, the results were also unsatisfied, the onset of the performance discontinuity wasn't predict correctly. In order to solve the problem of how to forecast the onset of discontinuity, the SST turbulence model is analysed.

The SST turbulence model combines the advantages of the k-ε and the k-ω turbulence model, and accounts for the transport of the turbulence shear stress. It gives highly accurate predictions of the onset and the amount of flow separation under adverse pressure gradients. Both the k-ε and the k-ω turbulence model do not account for the transport of the turbulent shear stress, thus they over predict the eddy-viscosity. The essential idea of the SST model is modifying the definition of the eddy-viscosity for adverse pressure gradient boundary-layer flow in much the same way as the Johnson-King model does[16]. Hence the SST model gives a new definition of the eddy-viscosity:

$$\mu_t = \frac{\rho a_1 k}{\max\left(a_1\omega, SF_2\right)} \tag{1}$$

Where F_2 is a blending function, which limits the modification to boundary-layer flows, i.e., in the boundary-layer the definition of the eddy-viscosity is:

$$\mu_t = \frac{\rho a_1 k}{SF_2} \tag{2}$$

In other domain the definition of the eddy-viscosity is:

$$\mu_t = \frac{\rho k}{\omega} \tag{3}$$

The middle span section of the impeller model is shown in Fig. 9. In the picture it only has two colours, the red part represents the eddy-viscosity was calculated by equation (3), and the blue part represents the eddy-viscosity was calculated by equation (2). The computational condition is Φ_2=0.164, the SST model used.

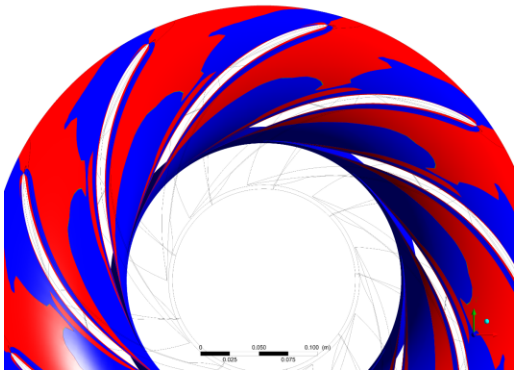

Figure 9. Distribution of the eddy-viscosity definitions

Fig.9 illustrates that the default blending function of the SST model does not succeed to limit equation (2) to boundary-layer flows. The equation (2) was still used in the core flow domain to calculate the eddy-viscosity, but Bradshaw's assumption doesn't necessarily hold in free shear-layer.

Thus the default blending function of the SST model isn't always suitable to the internal flow computation of the hydraulic machinery. But we noted that the effect of the blending function F_1 of the SST model is limiting the k-ω turbulence model to boundary-layer flows, and the effect of the blending function F_2 of the SST model is limiting the equation (2) to boundary-layer flows. Just because the modification to the eddy-viscosity has its largest impact in the wake region of the boundary layer, it is imperative that F_2 extends further out into the boundary-layer than F_1[16]. But F_2 was applied in the situation of the external flow originally, we don't know if it works well in the internal flow. Fig. 10 exhibits the distribution of F_1 and F_2 in the middle span section of the impeller.

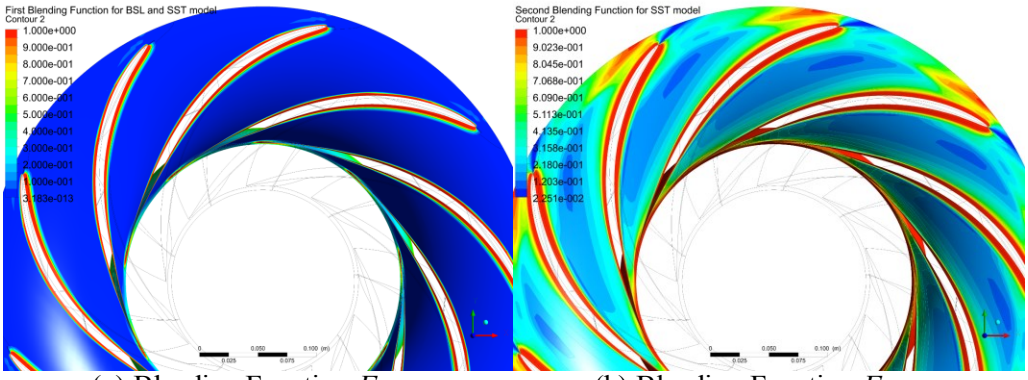

(a) Blending Function F_1 (b) Blending Function F_2

Figure 10. Distribution of F_1 and F_2

It can be found that the effective area of F_1 is limited to the boundary layer, and that of F_2 extends to the core of flow channels. We can know from Fig. 9 that the extension of F_2 resulted in the equation (2) activation in a large part of the core flow domain. It is unreasonable. So we used F_1 instead of F_2, i.e.:

$$\mu_t = \frac{\rho a_1 k}{\max\left(a_1\omega, SF_1\right)} \tag{4}$$

The distribution of the eddy-viscosity definitions in the middle span section of the impeller is shown in Fig. 11. The computational condition is Φ_2=0.155, the modified SST model used.

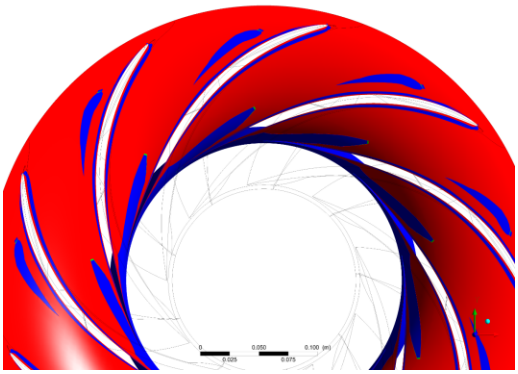

Figure 11. Distribution of the eddy-viscosity definitions

The red part represents the eddy-viscosity was calculated by equation (3) as well. The modified SST model control the distribution of the eddy-viscosity definitions well.

The Φ-ψ curve calculated by the modified SST model is shown in Fig. 12.

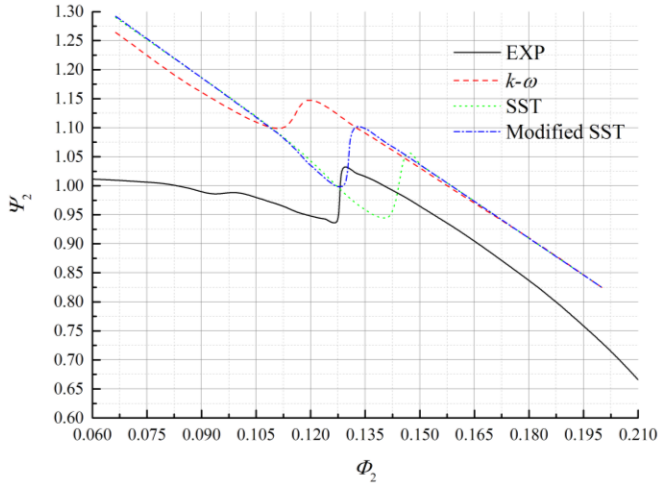

Figure 12. Φ-ψ curves

Fig.12 shows the results obtained from the modified SST model in comparison to the previous results. It is clearly presented that the ability to predict the onset of the performance discontinuity is improved using the modified SST model. We used the modified SST model to calculate other cases in order to predict the onset of performance discontinuity, and the modified SST model also works better than the k-ω model and the SST model. So this model gave us another method to predict the performance discontinuity correctly without increasing computational cost.

6. CONCLUSIONS

The present paper analyzed the phenomenon of performance discontinuity of a pump-turbine model under pumping mode by means of experiment and numerical simulation. Main conclusions are:

(1) The performance discontinuity point corresponds to the onset of inlet recirculation of impeller and the length of inlet recirculation decreases while the flowrate of operating condition increases.

(2) Pumping casing has little impact to the performance discontinuity, the impeller is the main driver.

(3) The modified SST model improves the ability to predict the onset of performance discontinuity of a pump-turbine.

ACKNOWLEDGMENTS

The authors would like to gratefully thank the ASTRÖ which is a hydraulic lab of ANDRITZ AG. This work is supported by Natural Science Foundation of China under the Grant No. 51379179, the Research Fund of the education department of Sichuan Province(No. 11ZB008) and the key project of Xihua University(No. z1120414).

References

[1] Greitzer E M 1980 The Stability of Pumping Systems - The 1980 Freeman Scholar Lecture *ASME J. Fluids Eng.* vol. **103** pp 193–242.

[2] Kaupert K A Holbein P and Staubli T 1996 A First Analysis of Flow Field Hysteresis in a Centrifugal Impeller *ASME J. Fluids Eng.* vol. **10** pp 685–691.

[3] Stoffel B 1989 Experimentelle Untersuchung zur raeumlichen und zeitlichen ruktur der Teillast-Rezirkulationen bei Kreiselpumpen *Forschung im Ingenieurwesen* Bd. **55** Nr 5.

[4] Pfleiderer C and Petermann H 1991 Stroemungsmaschinen *Springer-Verlag Heidelberg* 6th edition.

[5] Gülich J F 2008 Centrifugal Pumps *Berlin: Springer-Verlag Berlin Heidelberg*.

[6] Sinha M Pinarbasi A Katz J 2001 The flow structure during onset and developed states of rotating stall with in a vaned diffuser of a centrifugal pump *ASME J. Fluids Eng.* vol. **123(3)** pp 490-499.

[7] Sano T Yoshida Y Tsujimoto Y *et al* 2002 Numerical study of rotating stall in a pump vaned diffuser *ASME J. Fluids Eng*. vol. **124** pp 363-370.
[8] Wang H, Tsukamoto H 2003 Experimental and numerical study of unsteady flow in a diffuser pump at off-design conditions *ASME J. Fluids Eng*. vol. **125** pp 767-778.
[9] Ran H J Luo X W and Chen Y L *et al* 2012 Hysteresis phenomena in hydraulic measurement *26th IAHR Symposium on Hydraulic Machinery and Systems*.
[10] Braun O Kueny J L and Avellan F 2005 Numerical analysis of flow phenomena related to the unstable energy-discharge characteristic of a pump-turbine in pump mode *Proc. ASME FEDSC* vol. **1** part B pp 1075–1080.
[11] Kaupert K A Staubli T 1999 The Unsteady Pressure Field in a High Specific Speed Centrifugal Pump Impeller—Part II: Transient Hysteresis in the Characteristic *ASME J. Fluids Eng*. vol. **121** pp 627-632.
[12] Sedlái M Komárek M Vyroubal M *et al* 2013 Experimental and numerical analysis of unsteady behaviour of high efficiency mixed-flow pump *Experimental Fluid Mechanics*(02104).
[13] Eisele K Muggli F Zhang Z and Casey M V *et al* 1998 Experimental and Numerical Studies of Flow Instabilities in Pump-Turbine Stages *XIX IAHR Symposium Hydraulic Machinery and Cavitation*.
[14] Masamichi I Kazuhiro T Kazuyoshi M *et al* 2003 Numerical simulation of hysteresis on head/discharge characteristics of a centrifugal pump *Proc. ASME FEDSM'03 4th ASME-JSME Joint Fluids Eng. Conf.*(45399).
[15] Ginter F Staubli T 1999 Performance discontinuity of a shrouded centrifugal pump impeller: Part 1 – numerical model and flow instability *IMechE C*(557/080) pp 1027-1037.
[16] Menter F R 1992 Improved Two-Equation k-Turbulence Models for Aerodynamic Flows *NASA Technical Memorandum*(103975).
[17] Braun O, Avellan F and Dupont P 2007 Unsteady numerical simulations of the flow related to the unstable energy-discharge characteristic of a medium specific speed double suction pump *Proc. FEDSM2007 5th Joint ASME/JSME Fluids Eng. Conf.*(37550).